



Lysosome-targetable red-emitting ratiometric fluorescent probe for hypobromous acid imaging in living cells

Wangbo Qu^{a,c,1}, Kaibin Li^{a,1}, Deman Han^{a,**}, Xinxin Zhong^c, Caixia Chen^a, Xiuxia Liang^a, Heng Liu^{b,c,*}

^a Department of Chemistry, Taizhou University, Jiaojiang 318000, China

^b Institute of Functional Materials and Molecular Imaging, Key Laboratory of Emergency and Trauma, Ministry of Education, Key Laboratory of Hainan Trauma and Disaster Rescue, College of Clinical Medicine, College of Emergency and Trauma, Hainan Medical University, Haikou 571199, China

^c College of Chemistry and Chemical Engineering, Hubei University, Wuhan 430062, China

ARTICLE INFO

Keywords:

Hypobromous acid
Red-emitting
Ratiometric fluorescent probe
Fluorescence imaging

ABSTRACT

As one of the most important reactive oxygen species, hypobromous acid (HOBr) has been reported to be linked to a large body of diseases. Although some limited of HOBr-selective probes have been designed, there was no probes reported capable of sensing of HOBr with lysosome-targetable ability and red-emitting ratiometric fluorescence. Herein, we presented a 1,8-naphthalimide-based fluorescent probe Lyso-NpSN for rapid detection of HOBr over a wide pH range with high selectivity over other reactive oxygen species and sensitivity, for the first time. Furthermore, the probe was found to be low cytotoxicity to cells and had enabled to visualize exogenous and endogenous HOBr in living cells.

1. Introduction

Hypobromous acid (HOBr) is known as an important reactive oxygen species (ROS) in living biosystems generated by the reaction of bromide ions (Br^-) and hydrogen peroxide (H_2O_2) in the presence of eosinophil peroxidase (EPO) or myeloperoxidase (MPO) in vivo, having essential roles in immune response [1,2]. Growing evidences suggest that the high intracellular HOBr levels contributes to a diverse range of physiological and pathological processes caused by EPO disorders, including inflammatory, tissue damage, apoptosis, neurogenerative and cardiovascular diseases [3–6]. However, the blood plasma level of Br^- (2–100 μM) is approximately 1000-fold lower than that of Cl^- (100–140 mM), which leads to pose huge challenges in establishing effective analytical method for detection of HOBr [7–9]. As a result, the method for monitoring HOBr remains scarce.

Until present, due to its advantage of high sensitivity and non-invasive visualization, there have been a range of fluorescent probes for reactive oxygen species detection and imaging in living cells [10–16]. However, fluorescent probes capable of detecting HOBr were very limited. Han and co-workers have been first reported the two reversible near-infrared fluorescent probes for the determination of hypobromous acid/ascorbic acid and hypobromous acid/hydrogen sulfide on basis of

redox reaction [17,18]. Subsequently, Tang et al. reports two specific fluorescent probes BPP and RhSN-mito for native HOBr by HOBr-mediated coupling reaction of S-methyl and $-\text{NH}_2$ [19,20]. Based on this strategy, Tian et al. developed a mitochondria-targeted ratiometric fluorescent probe HAP for biosensing of HOBr [21]. However, the fluorescence signal of HAP locates in short-wavelength region (below 600 nm), which limits its application in bioimaging in living systems owing to autofluorescence of biomolecules [22–25].

Lysosome, a subcellular organelle found in eukaryotic cells containing many hydrolytic enzymes, has implicated in various cell processes, such as cell signaling, plasma membrane repair, energy metabolism [26,27]. It has been reported that lysosome function is closely related with ROS levels [28]. Recently, Zhang et al. have been developed a lysosome-targeted two-photon fluorescent probe NA-lyso for detecting HOBr, but NA-lyso is a single fluorescence signal on-off probe that has the drawbacks such as the lack of internal reference to eliminate errors [29,30]. Thus, it is still significative to construct long-wavelength lysosome-specific ratiometric fluorescent probes for HOBr detection and imaging.

Herein, we introduce the first red-emitting lysosome-targetable ratiometric fluorescent probe Lyso-NpSN for selective detection of HOBr. 1,8-naphthalimide was chosen as the fluorophore due to its excellent

* Corresponding author.

** Corresponding author.

E-mail addresses: hdmztc@126.com (D. Han), liuheng11b@hubu.edu.cn (H. Liu).

¹ These two authors contributed equally to this work (W.B. Qu and K.B. Li).

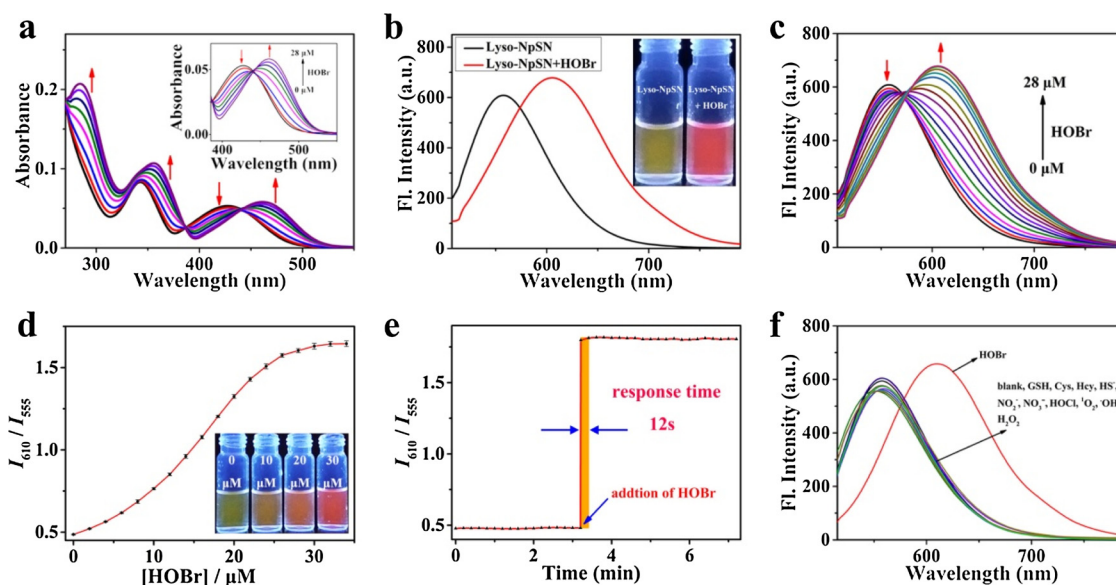
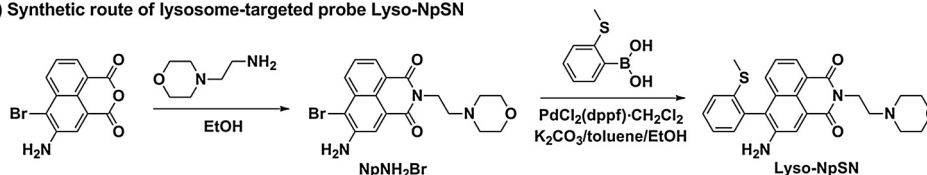
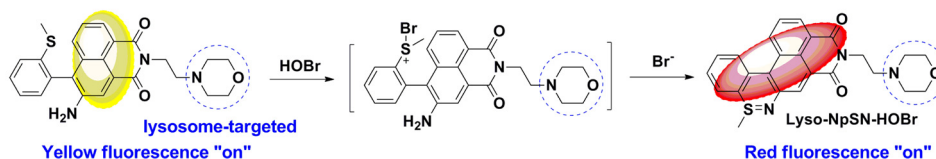


Fig. 1. (a) Absorption spectra of Lyso-NpSN upon treatment with HOBr (0–28 μM). (b) Fluorescence spectra of Lyso-NpSN before and after addition of 28 μM HOBr. Inset: photographs of Lyso-NpSN before and after addition of HOBr under UV irradiation. Fluorescence titration graph (c) and the ratio of fluorescence intensities (I_{610} / I_{555}) (d) of Lyso-NpSN upon different amounts of HOBr (0–28 μM). Inset: photographs of Lyso-NpSN upon different amounts of HOBr (0, 10, 20, 30 μM). (e) Time profile of ratiometric fluorescence signal (I_{610} / I_{555}) of Lyso-NpSN toward 28 μM HOBr. (f) Fluorescence spectra of Lyso-NpSN in the presence of HOBr (28 μM) and other ROS, RNS and RSS species. 200 μM for HClO, 500 μM for $^1\text{O}_2$, $\cdot\text{OH}$, H_2O_2 , $\text{NO}_2\cdot$, $\text{NO}_3\cdot$, 100 μM for NaSH, 1 mM GSH and 200 μM for Cys and Hcy.

(a) Synthetic route of lysosome-targeted probe Lyso-NpSN



(b) Proposed reaction mechanism of Lyso-NpSN with HOBr



Scheme 1. (a) Synthetic route of lysosome-targetable ratiometric fluorescent probe Lyso-NpSN; (b) Proposed reaction mechanism of lyso-NpSN with HOBr.

optical properties such as high photostability and quantum yield. Upon the reaction with HOBr, probe Lyso-NpSN showed a clear fluorescence color change with fluorescence red-shift from 555 nm to 610 nm. Further application demonstrated that Lyso-NpSN was capable of staining lysosome and imaging exogenous and endogenous HOBr in living cells.

2. Experimental section

2.1. Materials and instruments

All solvents used in this experiment were reagent grade. All solutions used in this experiment were prepared by Ultrapure water (18.2 M Ω cm). ^1H NMR and ^{13}C NMR were measured on a BRUKER 400 spectrometer using tetramethylsilane (TMS) as internal reference. HR-ESI-MS was performed using a Bruker ESI-TOF. All UV-vis absorption spectra were carried out on an Agilent Technologies Cary 60 UV-vis. Fluorescence spectra were measured on an Agilent Cary Eclipse fluorescence spectrophotometer. All fluorescence images of HeLa cells were obtained under a Leica SP8 STED 3X confocal fluorescence microscope.

2.2. Synthesis of NpNH₂Br

3-Amino-4-bromo-1,8-naphthalic anhydride (120 mg, 0.41 mmol) and 4-(2-aminoethyl) morpholine (106 mg, 0.82 mmol) were dissolved in ethanol (10 ml), and then the reaction was refluxed for 6 h. After the reaction was cooled to room temperature, the solid was slowly precipitated and washed with cold ethanol. The precipitate was filtered off and dried to give NpNH₂Br as a pale yellow solid (133 mg, 80.2%). ^1H NMR (400 MHz, d_6 -DMSO): δ 8.20 (d, $J = 8.4$ Hz, 1 H), 8.15 (d, $J = 7.2$ Hz, 1 H), 8.11 (s, 1 H), 7.76 (t, $J = 7.8$ Hz, 1 H), 6.32 (s, 2 H), 4.14 (t, $J = 7.0$ Hz, 2 H), 3.54–3.52 (m, 4 H), 2.55 (t, $J = 6.8$ Hz, 2 H), 2.46 (s, 4 H); ^{13}C NMR (400 MHz, d_6 -DMSO): δ 163.7, 163.5, 145.8, 132.0, 128.9, 126.3, 122.7, 122.4, 122.3, 121.7, 107.1, 66.7, 56.0, 53.9, 37.3; HR-ESI-MS m/z : $[\text{M}]^+$ calcd. for 404.0610 found 404.0609.

2.3. Synthesis of Lyso-NpSN

NpNH₂Br (80 mg, 0.198 mmol), 2-methylthiophenylboronic acid (50 mg, 0.297 mmol), Pd(dppf)₂Cl₂·CH₂Cl₂ (9 mg, 0.01 mmol), K₂CO₃ (4 M, 2 mL), EtOH (0.6 mL), toluene (5 mL) was added to a 50 mL round bottom flask, and the reaction was heated at 80 $^\circ\text{C}$ for 24 h under nitrogen atmosphere. After removing the solvent under reduced pressure,

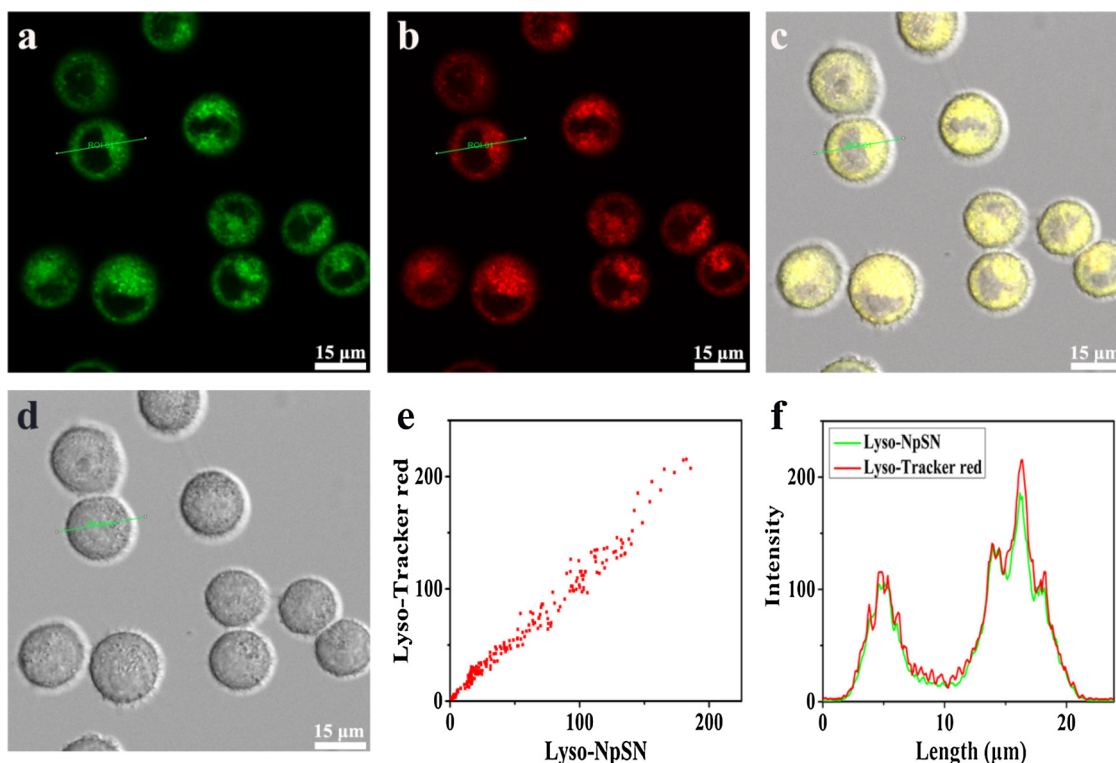


Fig. 2. Co-localization of Lyso-NpSN and Lyso-Tracker Red DND 99 in HeLa cells. Cells stained with Lyso-NpSN and Lyso-Tracker Red DND 99 for 30 min. (a) Green channel (500–555 nm); (b) Red channel (580–650 nm); (c) Overlap of (a) and (b); (d) Bright field; (e) Intensity correlation plot of Lyso-NpSN and Lyso-Tracker Red DND 99; (f) Intensity profile of linear region of interest across the HeLa cells in (c). (For interpretation of the references to colour in this figure legend, the reader is referred to the web version of this article).

the residue was purified by column chromatography ($\text{CH}_2\text{Cl}_2/\text{MeOH} = 50:1$) to give Lyso-NpSN as a grayish yellow solid (75.4 mg, 85.1%). ^1H NMR (400 MHz, CDCl_3): δ 8.25–8.23 (m, 1 H), 8.07 (s, 1 H), 7.47–7.32 (m, 4 H), 7.27–7.11 (m, 2 H), 4.29–4.26 (m, 2 H), 3.92 (s, 2 H), 3.64 (s, 4 H), 2.67–2.55 (m, 6 H), 2.29 (s, 3 H); ^{13}C NMR (400 MHz, CDCl_3): δ 164.6, 164.2, 142.8, 139.4, 132.6, 132.2, 130.8, 130.3, 129.6, 127.3, 127.2, 125.6, 125.0, 123.6, 123.2, 122.7, 122.5, 122.2, 67.0, 56.2, 53.8, 37.1, 15.0; HR-ESI-MS m/z : $[\text{M} + \text{H}]^+$ calcd. for 448.1695 found 448.1697.

2.4. General procedure for fluorescence measurement

A stock solution of 2 mM Lyso-NpSN was prepared in acetonitrile. The stock solution of hypobromous acid (HOBr) was prepared and quantitated according to a known method [31]. The solution of Lyso-NpSN with HOBr was prepared with 10 μL Lyso-NpSN stock solution, and appropriate volume of HOBr stock solution, and then were diluted to 2 mL with 10 mM PBS buffer- CH_3CN solution (3:2, v/v, pH 7.4). The fluorescence excitation wavelength was 475 nm with excitation and emission slits of 10 nm, and the emission was collected at 507–790 nm.

2.5. Co-localization experiments and fluorescence imaging of HOBr in living cells

HeLa cells were from the Institute of Biochemistry and Cell Biology, Shanghai Institutes for Biological Sciences, Chinese Academy of Sciences (Shanghai, China). HeLa cells were cultured in DMEM medium with 10% (v/v) fetal bovine serum albumin (FBS) and 1% (v/v) antibiotic (penicillin/streptomycin) in a 37 °C constant temperature and 5% CO_2 incubator. All HeLa cells were washed three times with PBS buffer solution (pH 7.4) before fluorescence image. Co-localization experiments in lysosome were performed using Lyso-NpSN and Lyso-Tracker Red DND 99 (a commercially available lysosomal red fluorescent dye).

HeLa cells were incubated with Lyso-NpSN (10 μM) and Lyso-Tracker Red DND 99 (75 nM) for 30 min at 37 °C. The fluorescence of Lyso-NpSN was collected in green channel (500–555 nm) with an excitation wavelength of 475 nm, and the fluorescence of Lyso-Tracker Red DND 99 was collected in red channel (580–650 nm) with an excitation wavelength of 577 nm. Finally, fluorescence images for HOBr in lysosomes were also studied. HeLa cells were incubated with Lyso-NpSN (10 μM), and then treated with HOBr (30 μM), NaBr (30 μM) or NaBr (30 μM)/N-acetylcysteine (20 μM). The fluorescence was collected in green channel (500–555 nm) and red channel (610–750 nm) with an excitation wavelength of 475 nm.

3. Results and discussion

3.1. Spectral response of Lyso-NpSN to HOBr

With the probe Lyso-NpSN in hand, we first evaluated its photo-physical properties in 10 mM PBS buffer- CH_3CN solution (3:2, v/v, pH 7.4) at 25 °C. Lyso-NpSN had two major absorption peaks centered at 340 nm and 425 nm. Upon increasing the amount of HOBr, three new strong absorption peaks centered at 283 nm, 340 nm and 460 nm appeared (Fig. 1a). The ratio of the two absorbance intensities (A_{460}/A_{425}) was linear with HOBr concentration in the range of 4–28 μM (linear equation: $y = 0.04561x + 0.4485$, $R^2 = 0.9989$) (Fig. S7, S8). As illustrated in Fig. 1b, free Lyso-NpSN displayed an emission peak at 555 nm under excitation at 475 nm. The fluorescence quantum yields of Lyso-NpSN was determined to be 0.25 using rhodamine B as a reference ($\phi_{\text{FL}} = 0.66$ in ethanol). In the presence of HOBr, a new emission peak at 610 nm emerged, accompanied by the emission peak at 555 nm decreased (Fig. 1c). Meanwhile, the color of the solution slowly turned from yellow to red under 365 nm UV irradiation with increasing amount of HOBr addition (Fig. 1d). What's more, the curve of fluorescence titration revealed that the ratio of fluorescence intensities (I_{610}

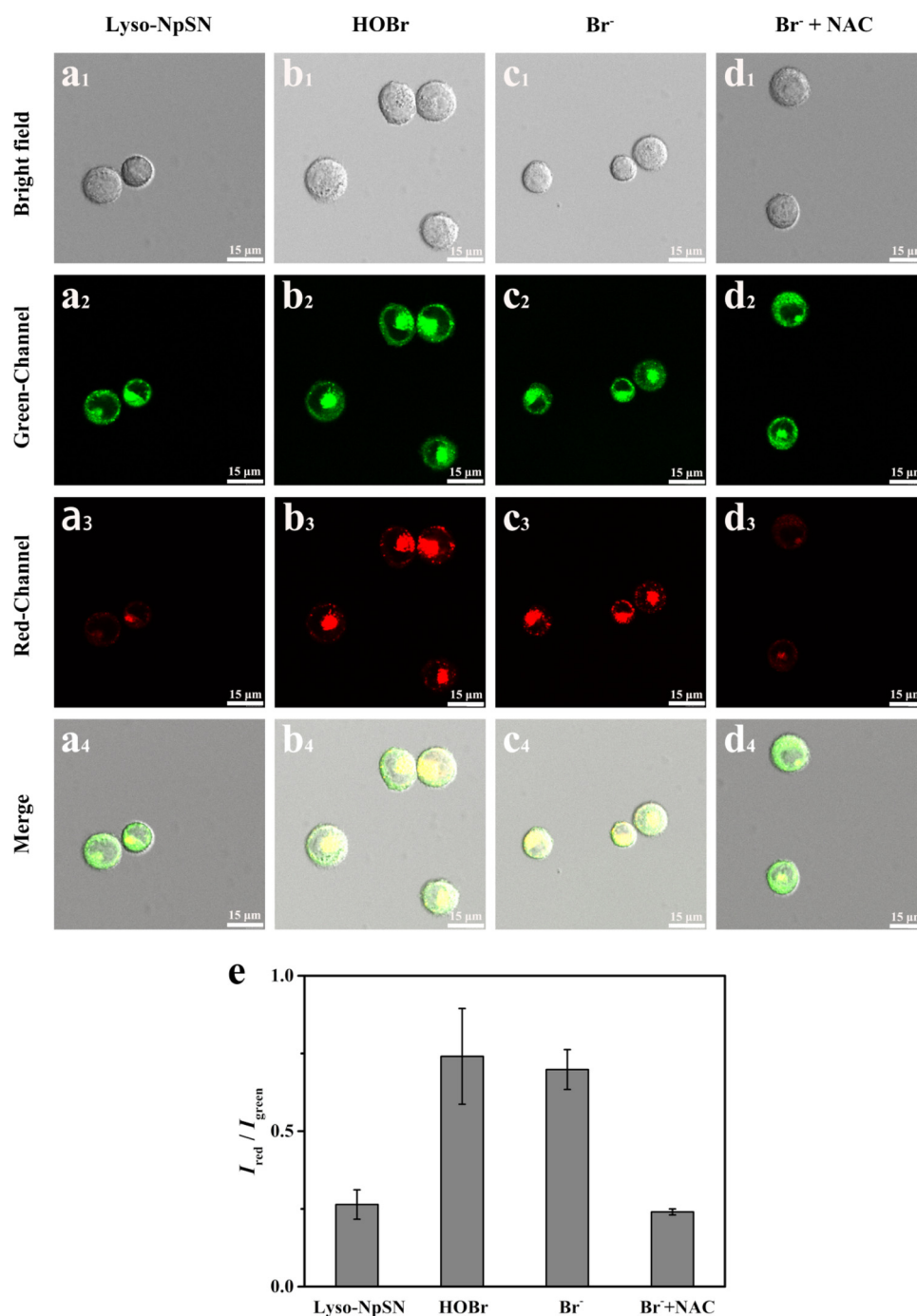


Fig. 3. Confocal fluorescence images of HeLa cells incubated with Lyso-NpSN (a), Lyso-NpSN and HOBr (b), Lyso-NpSN and Br⁻ (c), Lyso-NpSN and Br⁻/NAC (d). Green channel (500–555 nm), red channel (580–650 nm), $\lambda_{\text{ex}} = 475$ nm, scale bar = 15 μm. (e) Fluorescence intensity ratio ($I_{\text{red}} / I_{\text{green}}$) of cells in panels (a) to (d). (For interpretation of the references to colour in this figure legend, the reader is referred to the web version of this article).

I_{555}) had a good linearity with the concentration of HOBr in the range of 6–26 μM (linear equation: $y = 0.04916x + 0.4814$, $R^2 = 0.9836$) (Fig. 1d, S9). According to the formula $DL = 3\sigma/k$, the detection limit of Lyso-NpSN for HOBr was found to be as low as 99 nM. These results demonstrated that Lyso-NpSN was a highly sensitive ratiometric fluorescent probe for HOBr. Moreover, pH effect on the ratio of fluorescence intensities (I_{610} / I_{555}) of Lyso-NpSN in the presence or absence of HOBr was examined as well (Fig. S10). Free Lyso-NpSN was very stable over a wide pH range from 4.0 to 10.0. It was also observed that Lyso-NpSN showed an excellent response to HOBr in the pH range of 4.0–10.0, implying that Lyso-NpSN could be applied to detect HOBr with a stable fluorescence ratio signal output in a large pH range.

Next, the reaction kinetics of Lyso-NpSN toward HOBr was investigated. As shown in Fig. 1e and S11, the fluorescence intensity at 555 nm and ratio of fluorescence intensities (I_{610} / I_{555}) showed negligible change upon excitation at 475 nm in the absence of HOBr, revealing the photostability of the probe was very good. When 28 μM of HOBr was added to the solution, the ratio of fluorescence intensities (I_{610} / I_{555}) reached a stable value within 12 s. The response of Lyso-NpSN to HOBr was so fast that Lyso-NpSN held immense potential to be used in real-time monitoring of HOBr in living cells. To get better insight into the selectivity of Lyso-NpSN, the ratio of fluorescence intensities (I_{610} / I_{555}) changes were explored after addition of different biological potential interfering analytes. As depicted in Fig. S12, upon

adding different interfering metal cations (K^+ , Na^+ , Cu^{2+} , Zn^{2+} , Fe^{2+} , Fe^{3+}), anions (CO_3^{2-} , Ac^- , SO_4^{2-} , $S_2O_3^{2-}$, Br^-) and amino acids (Met, Pro, His, Ala, Thr, Leu) to the solution of Lyso-NpSN, negligible ratiometric fluorescence changes were observed. Furthermore, no distinct ratiometric fluorescence changes were triggered by the treatment with RSS (GSH, Cys, Hcy, HS $^-$), RNS (NO_2^- , NO_3^-) and ROS (HOCl, 1O_2 , $\cdot OH$, H_2O_2). Only adding HOBr to the solution of Lyso-NpSN switched a remarkable fluorescence shift change from 555 nm to 610 nm (Fig. 1f). Interestingly, HOBr showed different reaction pathway from HOCl with the probe Lyso-NpSN (Fig. S13 and S14). Moreover, the solution color of Lyso-NpSN incubated with HOBr showed red fluorescence under 365 nm UV irradiation while that of Lyso-NpSN in the presence or absence of other interfering analytes showed yellow fluorescence (Fig. S15).

Similar to the previously reported probes by Tang et al. [18,19], the fluorescence sensing response of Lyso-NpSN to HOBr underwent HOBr-mediated nucleophilic substitution and intramolecular cyclization reaction (Scheme 1b). To verify the sensing mechanism, the reaction product between Lyso-NpSN and HOBr was analyzed by HR-ESI-MS analysis. In Fig. S16, when Lyso-NpSN was treated with HOBr, the mixture showed the presence of peak at m/z 446.1548, which corresponded to Lyso-NpSN-HOBr occur. The reaction of Lyso-NpSN and HOBr was also performed, and the product Lyso-NpSN-HOBr was obtained with the yield of 60% (Fig. S17). The structure of Lyso-NpSN-HOBr was confirmed by NMR and MS.

3.2. Cell imaging

Prior to cell imaging applications, the cytotoxicity of Lyso-NpSN was firstly assessed using HeLa cells by CCK-8 assays (Fig. S21). The results revealed that when the concentration of Lyso-NpSN was below 20 μM , 91% cells were survived after incubation with Lyso-NpSN for 12 h. Subsequently, to demonstrate that Lyso-NpSN was capable of specific enrichment in lysosomes, co-localization experiments were performed by co-staining HeLa cells with Lyso-NpSN and commercial Lyso-Tracker Red DND 99 (Fig. 2). Fig. 2c showed that green signals from Lyso-NpSN and red signals from Lyso-Tracker Red DND 99 overlapped very well. From the intensity correlation plots, the Pearson's and overlap coefficient gave a value of 0.991 and 0.995, respectively, revealing Lyso-NpSN possessed excellent lysosomal targetable ability in living cells.

Thereafter, Lyso-NpSN was explored to image exogenous and endogenous HOBr in living HeLa cells. As demonstrated in Fig. 3a, the cells stained with Lyso-NpSN emitted strong green fluorescence and weak red fluorescence upon excitation at 475 nm. After treatment with exogenous HOBr, a marked 2.8-fold ratiometric fluorescence signal increase was obtained compared to the cells only incubated with Lyso-NpSN (Fig. 3b and Fig. 3e). Additionally, the cells incubated with Lyso-NpSN and stimulated by Br^- also triggered a significant increase in the ratio of mean fluorescence intensities in red and green channels from 0.26 to 0.69. In the presence of Br^- and N-Acetyl-L-cysteine (NAC, a reported scavenger of HOBr), a slight decrease in the ratio of mean fluorescence intensities was seen, showing the capability of Lyso-NpSN in ratiometrically imaging endogenous HOBr.

4. Conclusion

In summary, we have designed and synthesized the first red-emitting lysosome-targetable ratiometric fluorescent probe for imaging of HOBr. Significantly, Lyso-NpSN showed excellent selectivity and sensitivity toward HOBr and had a low detection limit of 99 nM. Co-localization experiments revealed that Lyso-NpSN could specifically stain in lysosome. Notably, Lyso-NpSN was capable of ratiometrically fluorescence imaging exogenous and endogenous HOBr in living cells. We believed that Lyso-NpSN would be a useful chemical tool for the understanding of the physiological effects of HOBr.

Acknowledgements

This work was supported by the National Natural Science Foundation of China (NSFC. 21575097, 21602051, 21804097), the Zhengjiang Provincial Natural Science Foundation of China (LQ18B050001), China Postdoctoral Science Foundation (2018M642402).

Appendix A. Supplementary data

Supplementary material related to this article can be found, in the online version, at doi:<https://doi.org/10.1016/j.snb.2019.126826>.

References

- [1] P.G. Furtmüller, U. Burner, G. Regelsberger, C. Obinger, Spectral and kinetic studies on the formation of eosinophil peroxidase compound I and its reaction with halides and thiocyanate, *Biochemistry* 39 (2000) 15578–15584.
- [2] W. Wu, Y. Chen, A. d'Avignon, S.L. Hazen, 3-Bromotyrosine and 3,5-dibromotyrosine are major products of protein oxidation by eosinophil peroxidase: potential markers for eosinophil-dependent tissue injury in vivo, *Biochemistry* 38 (1999) 3538–3548.
- [3] A.S. McCall, Christopher F. Cummings, G. Bhav, R. Vanacore, A. Page-McCaw, Billy G. Hudson, Bromine is an essential trace element for assembly of collagen IV scaffolds in tissue development and architecture, *Cell* 157 (2014) 1380–1392.
- [4] J. Wang, A. Slungaard, Role of eosinophil peroxidase in host defense and disease pathology, *Arch. Biochem. Biophys.* 445 (2006) 256–260.
- [5] B.A. Wagner, K.J. Reszka, M.L. McCormick, B.E. Britigan, C.B. Ewig, C. Patrick Burns, Role of thiocyanate, bromide and hypobromous acid in hydrogen peroxide-induced apoptosis, *Free. Radic. Res.* 38 (2004) 167–175.
- [6] S. Weiss, S. Test, C. Eckmann, D. Roos, S. Regiani, Brominating oxidants generated by human eosinophils, *Science* 234 (1986) 200–203.
- [7] H.A. Olszowy, J. Rossiter, J. Hegarty, P. Geoghegan, M. Haswell-Elkins, Background levels of bromide in human blood, *J. Anal. Toxicol.* 22 (1998) 225–230.
- [8] P.G. Furtmüller, U. Burner, C. Obinger, Reaction of myeloperoxidase compound I with chloride, bromide, iodide, and thiocyanate, *Biochemistry* 37 (1998) 17923–17930.
- [9] F.X.R. van Leeuwen, B. Sangster, A.G. Hildebrandt, The toxicology of bromide ion, *CRC Crit. Rev. Toxicol.* 18 (1987) 189–213.
- [10] H. Tong, Y. Zhang, S. Ma, M. Zhang, N. Wang, R. Wang, et al., A pinacol boronate caged NIAD-4 derivative as a near-infrared fluorescent probe for fast and selective detection of hypochlorous acid, *Chin. Chem. Lett.* 29 (2018) 139–142.
- [11] J.P. Li, S. Xia, H. Zhang, G.R. Qu, H.M. Guo, Three-input “AND-Type” fluorescent logic gate as ratio probe for specific imaging of hypochlorite in rough endoplasmic reticulum, *Sens. Actuators B-Chem.* 255 (2018) 622–629.
- [12] J. Li, X. Yang, D. Zhang, Y. Liu, J. Tang, Y. Li, et al., A fluorescein-based “turn-on” fluorescence probe for hypochlorous acid detection and its application in cell imaging, *Sens. Actuators B-Chem.* 265 (2018) 84–90.
- [13] Z. Lou, P. Li, K. Han, Redox-responsive fluorescent probes with different design strategies, *Acc. Chem. Res.* 48 (2015) 1358–1368.
- [14] B. Zhang, X. Yang, R. Zhang, Y. Liu, X. Ren, M. Xian, et al., Lysosomal-targeted two-photon fluorescent probe to sense hypochlorous acid in live cells, *Anal. Chem.* 89 (2017) 10384–10390.
- [15] F. Yu, P. Li, B. Wang, K. Han, Reversible near-infrared fluorescent probe introducing tellurium to mimetic glutathione peroxidase for monitoring the redox cycles between peroxynitrite and glutathione in vivo, *J. Am. Chem. Soc.* 135 (2013) 7674–7680.
- [16] F. Yu, P. Li, G. Li, G. Zhao, T. Chu, K. Han, A near-irreversible fluorescent probe modulated by selenium for monitoring peroxynitrite and imaging in living cells, *J. Am. Chem. Soc.* 133 (2011) 11030–11033.
- [17] B. Wang, P. Li, F. Yu, J. Chen, Z. Qu, K. Han, A near-infrared reversible and ratiometric fluorescent probe based on Se-BODIPY for the redox cycle mediated by hypobromous acid and hydrogen sulfide in living cells, *Chem. Commun.* 49 (2013) 5790–5792.
- [18] F. Yu, P. Song, P. Li, B. Wang, K. Han, Development of reversible fluorescence probes based on redox oxoammonium cation for hypobromous acid detection in living cells, *Chem. Commun.* 48 (2012) 7735–7737.
- [19] X. Liu, A. Zheng, D. Luan, X. Wang, F. Kong, L. Tong, et al., High-quantum-yield mitochondria-targeting near-infrared fluorescent probe for imaging native hypobromous acid in living cells and in vivo, *Anal. Chem.* 89 (2017) 1787–1792.
- [20] K. Xu, D. Luan, X. Wang, B. Hu, X. Liu, F. Kong, et al., An ultrasensitive cyclization-based fluorescent probe for imaging native HOBr in live cells and zebrafish, *Angew. Chem. Int. Ed.* 55 (2016) 12751–12754.
- [21] H. Huang, Y. Tian, A ratiometric fluorescent probe for bioimaging and biosensing of HBrO in mitochondria upon oxidative stress, *Chem. Commun.* 54 (2018) 12198–12201.
- [22] W. Qu, C. Niu, X. Zhang, W. Chen, F. Yu, H. Liu, et al., Construction of a novel far-red fluorescence light-up probe for visualizing intracellular peroxynitrite, *Talanta* 197 (2019) 431–435.
- [23] D. Wu, L. Chen, W. Lee, G. Ko, J. Yin, J. Yoon, Recent progress in the development of organic dye based near-infrared fluorescence probes for metal ions, *Coord. Chem.*

- Rev. 354 (2018) 74–97.
- [24] X. Han, X. Song, B. Li, F. Yu, L. Chen, A near-infrared fluorescent probe for sensitive detection and imaging of sulfane sulfur in living cells and in vivo, *Biomater. Sci.* 6 (2018) 672–682.
- [25] J. Chin, H.J. Kim, Near-infrared fluorescent probes for peptidases, *Coord. Chem. Rev.* 354 (2018) 169–181.
- [26] P. Saftig, J. Klumperman, Lysosome biogenesis and lysosomal membrane proteins: trafficking meets function, *Nat. Rev. Mol. Cell. Biol.* 10 (2009) 623.
- [27] G. Kroemer, M. Jäättelä, Lysosomes and autophagy in cell death control, *Nat. Rev. Cancer* 5 (2005) 886.
- [28] T. Kurz, A. Terman, B. Gustafsson, U.T. Brunk, Lysosomes and oxidative stress in aging and apoptosis, *BBA-Gen. Subj.* 1780 (2008) 1291–1303.
- [29] C. Ma, M. Ma, Y. Zhang, X. Zhu, L. Zhou, R. Fang, et al., Lysosome-targeted two-photon fluorescent probe for detection of hypobromous acid in vitro and in vivo, *Spectrochim. Acta A. Mol. Biomol. Spectrosc.* 212 (2019) 48–54.
- [30] W. Qu, X. Zhang, Y. Ma, F. Yu, H. Liu, A novel near-infrared fluorescent probe for detection of hypobromous acid and its bioimaging applications, *Spectrochim. Acta A. Mol. Biomol. Spectrosc.* 222 (2019) 117240.
- [31] K. Kumar, D.W. Margerum, Kinetics and mechanism of general-acid-assisted oxidation of bromide by hypochlorite and hypochlorous acid, *Inorg. Chem.* 26 (1987) 2706–2711.